

# Lawrence Berkeley National Laboratory

## LBL Publications

### Title

Triaxiality near the 110Ru ground state from Coulomb excitation

### Permalink

<https://escholarship.org/uc/item/92k254g8>

### Authors

Doherty, DT  
Allmond, JM  
Janssens, RVF  
[et al.](#)

### Publication Date

2017-03-01

### DOI

10.1016/j.physletb.2017.01.031

Peer reviewed



## Triaxiality near the $^{110}\text{Ru}$ ground state from Coulomb excitation



D.T. Doherty<sup>a,\*</sup>, J.M. Allmond<sup>b</sup>, R.V.F. Janssens<sup>c</sup>, W. Korten<sup>a</sup>, S. Zhu<sup>c</sup>, M. Zielińska<sup>a</sup>, D.C. Radford<sup>b</sup>, A.D. Ayangeakaa<sup>c</sup>, B. Bucher<sup>d</sup>, J.C. Batchelder<sup>e</sup>, C.W. Beausang<sup>f</sup>, C. Campbell<sup>g</sup>, M.P. Carpenter<sup>c</sup>, D. Cline<sup>h</sup>, H.L. Crawford<sup>i</sup>, H.M. David<sup>c</sup>, J.P. Delaroche<sup>j</sup>, C. Dickerson<sup>c</sup>, P. Fallon<sup>g</sup>, A. Galindo-Uribarri<sup>b,k</sup>, F.G. Kondev<sup>c</sup>, J.L. Harker<sup>l,c</sup>, A.B. Hayes<sup>h</sup>, M. Hendricks<sup>c</sup>, P. Humby<sup>f</sup>, M. Girod<sup>j</sup>, C.J. Gross<sup>b</sup>, M. Klintefjord<sup>b,m</sup>, K. Kolos<sup>k</sup>, G.J. Lane<sup>n</sup>, T. Lauritsen<sup>c</sup>, J. Libert<sup>j</sup>, A.O. Macchiavelli<sup>g</sup>, P.J. Napiorkowski<sup>o</sup>, E. Padilla-Rodal<sup>p</sup>, R.C. Pardo<sup>c</sup>, W. Reviol<sup>q</sup>, D.G. Sarantites<sup>q</sup>, G. Savard<sup>c</sup>, D. Seweryniak<sup>c</sup>, J. Srebrny<sup>o</sup>, R. Varner<sup>b</sup>, R. Vondrasek<sup>c</sup>, A. Wiens<sup>g</sup>, E. Wilson<sup>f</sup>, J.L. Wood<sup>r</sup>, C.Y. Wu<sup>d</sup>

<sup>a</sup> Irfu, CEA, Université Paris-Saclay, F-91191 Gif-sur-Yvette, France

<sup>b</sup> Physics Division, Oak Ridge National Laboratory, Oak Ridge, TN 37831, USA

<sup>c</sup> Physics Division, Argonne National Laboratory, Argonne, IL 60439, USA

<sup>d</sup> Lawrence Livermore National Laboratory, Livermore, CA 94550, USA

<sup>e</sup> Department of Nuclear Engineering, University of California, Berkeley, Berkeley CA 94702, USA

<sup>f</sup> Department of Physics, University of Richmond, Richmond, VA 23173, USA

<sup>g</sup> Nuclear Science Division, Lawrence Berkeley National Laboratory, Berkeley, CA 94720, USA

<sup>h</sup> Department of Physics and Astronomy, University of Rochester, Rochester, NY 14627, USA

<sup>i</sup> Ohio University, Athens, OH 45701, USA

<sup>j</sup> CEA, DAM, DIF, F-91297 Arpajon, France

<sup>k</sup> Department of Physics and Astronomy, University of Tennessee, Knoxville, TN 37996, USA

<sup>l</sup> Department of Chemistry and Biochemistry, University of Maryland, College Park, MD 20742, USA

<sup>m</sup> Department of Physics, University of Oslo, Oslo, N-0316, Norway

<sup>n</sup> Department of Nuclear Physics, Research School of Physical Science and Engineering, Australian National University, Canberra, ACT 0200, Australia

<sup>o</sup> Heavy Ion Laboratory, University of Warsaw, Warsaw, Poland

<sup>p</sup> Instituto de Ciencias Nucleares, UNAM, AP 70-543, 04510 Mexico, D.F., Mexico

<sup>q</sup> Department of Chemistry, Washington University, St. Louis, MO 63130, USA

<sup>r</sup> School of Physics, Georgia Institute of Technology, Atlanta, GA 30332-0430, USA

### ARTICLE INFO

#### Article history:

Received 22 October 2016

Received in revised form 14 December 2016

Accepted 17 January 2017

Available online 20 January 2017

Editor: D.F. Geesaman

### ABSTRACT

A multi-step Coulomb excitation measurement with the GRETINA and CHICO2 detector arrays was carried out with a 430-MeV beam of the neutron-rich  $^{110}\text{Ru}$  ( $t_{1/2} = 12$  s) isotope produced at the CARIBU facility. This represents the first successful measurement following the post-acceleration of an unstable isotope of a refractory element. The reduced transition probabilities obtained for levels near the ground state provide strong evidence for a triaxial shape; a conclusion confirmed by comparisons with the results of beyond-mean-field and triaxial rotor model calculations.

© 2017 The Authors. Published by Elsevier B.V. This is an open access article under the CC BY license (<http://creativecommons.org/licenses/by/4.0/>). Funded by SCOAP<sup>3</sup>.

The shape is a fundamental property of the atomic nucleus and, while the majority of nuclei are thought to be axially symmetric, triaxial deformation has been a subject of much recent interest in structure studies. So far, triaxial deformation has been established to occur in specific nuclei at high angular momenta [1–3] through either the wobbling motion [4] or the breaking of chiral

symmetry [5] under rotation. Furthermore, its presence at or near the ground state has been studied extensively in the past, primarily via Coulomb excitation of stable nuclei [6–9], without reaching definitive conclusions for any region of the nuclear chart as the nuclei involved are more commonly viewed as “ $\gamma$ -soft” rather than as rigidly triaxial. In addition to the general question of whether nuclei can exhibit these exotic shapes, this issue is particularly intriguing given the anticipated influence on nuclear binding energies and thus on a number of astrophysical processes [10,11]. The results of several microscopic calculations indicate that the

\* Corresponding author.

E-mail address: [d.t.doherty@surrey.ac.uk](mailto:d.t.doherty@surrey.ac.uk) (D.T. Doherty).

neutron-rich molybdenum and ruthenium isotopes are among the nuclei with the best prospects for the observation of low-spin triaxial phenomena, mainly due to the occupation of the neutron  $1\nu h_{11/2}$  and proton  $1\pi g_{9/2}$  intruder orbitals [12–16]. However, this is a challenging issue to address as the shape degrees of freedom ( $\beta$ ,  $\gamma$ , etc.) are defined in the intrinsic frame of the nucleus whereas observations are made in the laboratory, and one has to rely on the Kumar–Cline sum rules [17,18], which require knowledge of several experimental E2 matrix elements, to provide the bridge between the two.

The level structure of  $^{110,112}\text{Ru}$  has been investigated by prompt  $\gamma$ -ray spectroscopy of fission fragments [19–24] and in beta decay [25,26]. The excitation energy of the first  $2^+$  state reaches a near constant value between  $^{108}\text{Ru}$  and  $^{114}\text{Ru}$ ; i.e., close to the  $N = 66$  mid-shell point, suggesting constant quadrupole deformation. However, the ratio between the excitation energies of the first  $2^+$  and  $4^+$  states never reaches the rotational limit for axial symmetry ( $R_{42} = 10/3$ ), in contrast to the observations in the neighboring Sr and Zr isotopes. In addition, it has been shown that the energy of the  $2^+$  states decreases with increasing neutron number for the Ru isotopes, thus indicating an increasing susceptibility to the triaxial (or  $\gamma$ ) degree of freedom. In  $^{110}\text{Ru}$ , the  $2^+$  level is observed to be energetically below the  $4^+$  state, a strong indication of triaxiality according to the Rigid Triaxial Rotor Model (RTRM) of Davydov et al. [27,28]. In fact, the Mo–Ru isotopes have the lowest known  $2^+$  states of any nucleus, with the exception of  $^{192}\text{Os}$  [29]. In addition, the relation  $E(3^+) = E(2^+_1) + E(2^+_2)$ , indicating a possible breaking of axial symmetry, is satisfied in  $^{110-114}\text{Ru}$ . It is important to note that such empirical criteria for triaxiality are only fulfilled in one other area of the nuclear chart; i.e., in the neutron-rich Os and Pt isotopes [6], but in this case the phenomenon is limited to only a few isotopes, in contrast to a sizeable region.

Nevertheless, indisputable evidence for stable, non-axial nuclear shapes close to the ground state based solely on the analysis of energy spectra is notoriously difficult to obtain [30]. It is more instructive, therefore, to consider reduced transition probabilities in this type of analysis. Complications arise as  $B(E2)$  values or transition quadrupole moments in the ground-state band are only weakly affected by gamma deformation [31], although a recent study [32] reported such moments in the 8–16 $\hbar$  spin range for the yrast bands in  $^{108-112}\text{Ru}$  and discussed the results in terms of  $\gamma$  softness or possible triaxiality. More sensitive indications of triaxiality are the static quadrupole moments and the  $B(E2)$  reduced transition probabilities between levels of an excited,  $K = 2$ , band and states in the ground-state band [31]. In particular, Hartree–Fock–Bogolyubov (HFB) based calculations going beyond the mean-field approach using the Generator Coordinate Method (GCM) with the Gaussian Overlap Approximation (GOA), as well as results obtained with phenomenological triaxial rotor models [27,28] predict reduced quadrupole moments and large  $B(E2; J \rightarrow J)$  values between  $\Delta K = 2$  bands. For the ruthenium isotopes, however, such absolute  $B(E2)$  values between bands were thus far experimentally unknown beyond stable  $^{104}\text{Ru}$ , which was found to be characterized by a prolate-triaxial shape with a degree of  $\gamma$ -softness [7].

In this Letter, results from the first multi-step Coulomb excitation study of  $^{110}\text{Ru}$  are reported with the aim of searching for evidence of a triaxial shape close to the ground state, and of herewith providing new information on shape evolution in the Ru isotopes. This unique study represents the first post-acceleration of an unstable, isotope of a refractory element and can only now be realized thanks to the CARIBU facility [33]. Despite long-standing interest, such studies have hitherto been impossible due to the physical properties of refractory metals, which prevent their release from the targets used at traditional isotope separation on-

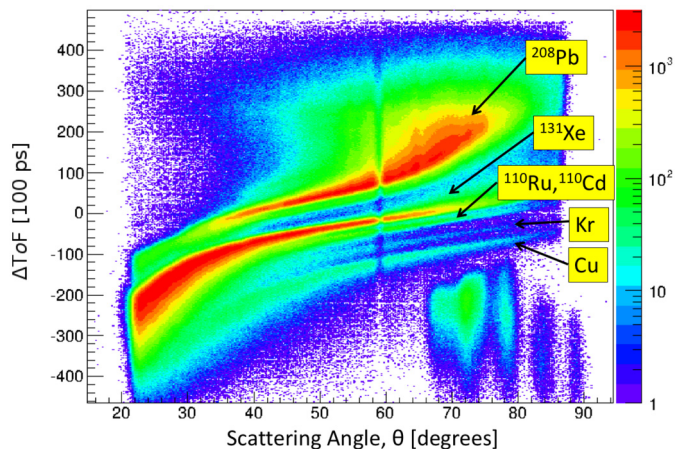


Fig. 1. (Color online.) The CHICO2 particle spectrum. The plot displays the difference in ToF between the beam and target nuclei versus scattering angle,  $\theta$ . The Pb recoils and various beam contaminants are labeled.

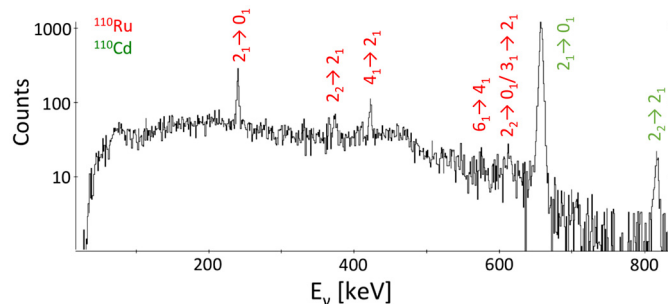
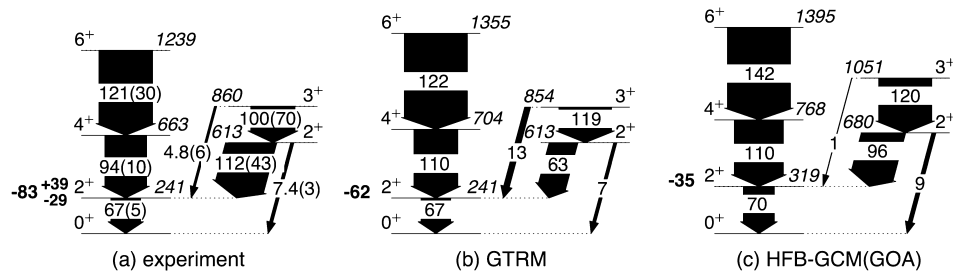


Fig. 2. (Color online.) Doppler corrected  $\gamma$ -ray energy spectrum gated on the  $A=110$  group in the CHICO2 spectrum. A number of  $^{110}\text{Cd}$  peaks (labeled in green) are visible in addition to the  $^{110}\text{Ru}$   $\gamma$  rays (red).

line (ISOL) facilities [33,34]. Furthermore, the measurement reported here also benefits from the superior Doppler reconstruction achieved by the combination of the  $\gamma$ -ray tracking capabilities of the GRETINA array [35] and a highly-segmented particle detector, CHICO2 [36].

The experiment was performed at the Argonne Tandem Linac Accelerator System (ATLAS). As stated above, the  $^{110}\text{Ru}$  beam was provided by the CARIBU facility [33,38,39] where, starting from a  $\sim 1.7\text{Ci}$   $^{252}\text{Cf}$  source, fission fragments were efficiently thermalized and turned into a beam of  $1^+$  charged ions by a gas catcher. The  $^{110}\text{Ru}^{1+}$  ions were then selected through the isobar separator and directed to a dedicated ECR source for charge breeding (to  $q = 21^+$ ) before being sent to the ATLAS linac for subsequent acceleration to 430 MeV. The  $^{110}\text{Ru}$  beam impinged on a 1.5  $\text{mg}/\text{cm}^2$ -thick  $^{208}\text{Pb}$  target (99.9% enrichment) located at the center of the GRETINA + CHICO2 experimental apparatus. The intensity of the radioactive beam was monitored at the beam dump by measuring the yield of  $\gamma$  rays associated with its beta decay (see Ref. [37] for details). On average, 2000  $^{110}\text{Ru}$  ions per second hit the target. Gamma rays from multi-step Coulomb excitation were measured by the GRETINA tracking array [35] in coincidence with scattered reaction partners detected in the CHICO2 heavy-ion counter [36]. For this experiment, GRETINA consisted of 8 modules with 4 segmented HPGe detectors each. Otherwise the experimental apparatus was essentially identical to that described in Ref. [37]. With the described setup, a resolution of 4.5 keV was achieved for the 658-keV transition in  $^{110}\text{Cd}$ , which is shown in Fig. 2.

A representative time-of-flight (ToF) particle histogram is given in Fig. 1 while a  $\gamma$ -ray spectrum gated on mass 110 reaction prod-



**Fig. 3.** Comparison between (a) the experimental, (b) GTRM and (c) HFB-GCM(GOA) level schemes of  $^{110}\text{Ru}$ . The excitation energies (in keV) and spin-parity values are given above the states. The widths and labels of the arrows represent the measured and calculated reduced  $E2$  transition probabilities in W.u. The experimental and theoretical spectroscopic quadrupole moments,  $Q_s$ , in  $e\text{ fm}^2$ , are given in bold next to the  $2_1^+$  states.

ucts is presented in Fig. 2. Contaminants; i.e., stable beams with a  $A/q$  ratio close to that of the desired  $^{110}\text{Ru}$  projectiles, can be readily identified in Fig. 1, but the temporal and spatial resolutions of CHICO2 were sufficient to separate all but the  $A=110$  isobars from the composite beam, as demonstrated by the coincident  $\gamma$ -ray spectrum (Fig. 2).

Unfortunately, these contaminants add to the complexity of the spectrum; in particular, the 658-keV,  $2^+ \rightarrow 0^+$  ground-state transition of  $^{110}\text{Cd}$  generates a significant contribution to the background under all the  $^{110}\text{Ru}$  lines of interest (due to Compton scattering). Nevertheless,  $^{110}\text{Ru}$  transitions from the yrast sequence up to the  $6^+$  state and from the  $2^+$  and  $3^+$  levels of the  $K^\pi = 2^+$  gamma band were identified and analyzed. It is worth noting that, due to the  $\gamma$ -ray tracking capabilities of GREINA [35], particular care was devoted to the determination of the energy dependence of the efficiency of the array. For this purpose, the detection efficiency was determined under tracking conditions identical to those used in the experiment with standard  $^{60}\text{Co}$ ,  $^{137}\text{Cs}$ ,  $^{152}\text{Eu}$  and  $^{182}\text{Ta}$  sources. Furthermore, in order to validate the tracking algorithms, the ratios between the intensities of the strongest  $^{110}\text{Ru}$  and  $^{110}\text{Cd}$  transitions measured in the tracked spectrum of Fig. 2 were found to be essentially identical to those extracted from the corresponding spectrum prior to tracking.

For the Coulomb excitation analysis,  $\gamma$ -ray yields were extracted for three separate ranges of the particle scattering angle;  $30^\circ$ – $40^\circ$ ,  $40^\circ$ – $60^\circ$  and  $60^\circ$ – $75^\circ$  in order to exploit the angular dependence of the excitation probabilities. Peak fitting was substantially aided by prior knowledge of the  $\gamma$ -ray energies [29], particularly for the analysis of the 613/619-keV doublet seen in Fig. 2. The yields were then corrected for detection efficiency and analyzed with the semi-classical Coulomb excitation code GOSIA [40], which allows extraction of the electromagnetic matrix elements from Coulomb excitation data by applying a fitting routine to the measured  $\gamma$ -ray intensities with these elements as parameters. In addition, known spectroscopic data such as lifetimes and branching ratios were included as further constraints of the relevant parameters during the fitting process. A set of matrix elements was then determined in the minimization process that reproduces within  $\sim 1\sigma$  all of the experimental  $\gamma$ -ray yields, as well as other known spectroscopic data. In the present analysis, states up to the  $8^+$  level in the ground-state sequence, the  $4^+$  in the  $K^\pi = 2^+$  gamma band and the first excited  $0^+$  state were considered together with their associated matrix elements. Lifetimes of the  $4^+$  and  $6^+$  states in the ground-state band were adopted from the most recent data evaluation [29], while the  $8^+$  lifetime is from Refs. [32,41]. The lifetime of the  $2_1^+$  state in  $^{110}\text{Ru}$  is discussed in detail below. Branching ratios were obtained from Ref. [25]. Unfortunately, information on  $E2/M1$  ratios for mixed transitions in  $^{110}\text{Ru}$  is currently not available. As a result, the  $2_2^+ \rightarrow 2_1^+$ ,  $3_1^+ \rightarrow 2_1^+$  and  $3_1^+ \rightarrow 2_2^+$  matrix elements (Table 1 and Fig. 3) assume pure  $E2$  transitions, in agreement with data for such mixing ratios mea-

**Table 1**

Experimental reduced transition probabilities between low-lying states in  $^{110}\text{Ru}$ , determined from the GOSIA fit to the experimental data, together with the results obtained with the two theoretical approaches discussed in the text. The bottom section of the table displays the spectroscopic quadrupole moment,  $Q_s$ , determined for the  $2_1^+$  level in the present work (see text for details).

$I_f^\pi \rightarrow I_i^\pi$	$E_\gamma$ (keV)	$B(E2; I_f \rightarrow I_i)$ ( $e^2b^2$ )		
		Experiment	GTRM	HFB-GCM(GOA)
$2_1^+ \rightarrow 0_1^+$	241	$0.209^{(+0.015, -0.016)}$	0.209	0.218
$4_1^+ \rightarrow 2_1^+$	423	$0.293^{(+0.031, -0.021)}$	0.309	0.344
$6_1^+ \rightarrow 4_1^+$	576	$0.38^{(+0.09, -0.04)}$	0.38	0.45
$2_2^+ \rightarrow 2_1^+$	372	$0.35^{(+0.13, -0.13)}$	0.20	0.30
$2_2^+ \rightarrow 0_1^+$	613	$0.023^{(+0.001, -0.001)}$	0.023	0.028
$3_1^+ \rightarrow 2_2^+$	247	$0.31^{(+0.21, -0.22)}$	0.37	0.38
$3_1^+ \rightarrow 2_1^+$	619	$0.015^{(+0.002, -0.002)}$	0.041	0.003
$I_i^\pi$		$Q_s$ ( $e\text{ fm}^2$ )		
$2_1^+$		$-83^{(+39, -29)}$	-62	-35

sured in the less neutron-rich members of the Ru isotopic chain [29]. Furthermore, including  $M1$  admixtures has a negligible influence on the excitation probabilities as  $E2$  transitions dominate in low-energy Coulomb excitation. Specifically, including an  $M1$  component in the  $2_2^+ \rightarrow 2_1^+$  decay, which is discussed below, reduces the lifetimes of the  $2_2^+$  level and acts to further reduce the already small  $2_2^+ \rightarrow 0_1^+$  matrix element, but does not influence the conclusions of the present paper.

The lifetime of the  $2_1^+$  state in  $^{110}\text{Ru}$  was not included in the analysis since a survey of the literature [42–44] reveals a rather large spread in the reported value for this level, raising some doubt as to the one to adopt. Specifically, a measurement following neutron-induced fission of  $^{249}\text{Cf}$  [43] reports a value significantly larger than that deduced elsewhere. The conversion of measured  $\gamma$ -ray intensities to absolute excitation cross sections was, therefore, achieved using only the lifetimes of the  $4^+$  and  $6^+$  states. With this procedure, an independent measurement of the lifetime of the  $2_1^+$  yrast level in  $^{110}\text{Ru}$  can then be deduced from the analysis: the measured 0.46(3) ns value agrees with that adopted in the recent compilation of Ref. [29]. In order to further reduce the number of free parameters in the GOSIA fit, measured intensities and accurately known  $B(E2)$  values for specific transitions in  $^{110}\text{Cd}$ , a stable contaminant in the beam, were used to determine the relative normalization between data sets from the three angular ranges. A detailed analysis similar to that for  $^{110}\text{Ru}$  was also carried out for all other transitions between low-lying states in  $^{110}\text{Cd}$ . Good agreement with the literature was found in all cases, specifically the extracted  $B(E2)$  values for the decay of the  $2_1^+$ ,  $2_2^+$ , and  $4_1^+$  levels are consistent with the compiled values [29] as is the

spectroscopic moment for the  $2_1^+$  state. This provides confidence in the analysis procedures and in the results discussed below.

The reduced transition probabilities are presented in Table 1 together with their associated uncertainties. Table 1 also provides the extracted spectroscopic quadrupole moment,  $Q_s$ , for the  $2_1^+$  state. Note that the  $3_1^+ \rightarrow 2_2^+$  transition is weak and was not directly observed in the spectra. Nevertheless, a transition probability could be derived with confidence from the GOSIA fit, based on the  $3_1^+ \rightarrow 2_1^+$  transition intensity measured in the present experiment and on the published branching ratio [25].

In order to aid in the interpretation of the experimental results, extensive beyond-mean-field calculations using the HFB-GCM(GOA) approach [45] with the Gogny D1S force [46,47] as well as calculations with the Generalized Triaxial Rotor Model (GTRM) [48–51] have been performed for  $^{110}\text{Ru}$ . The results are also presented in Table 1, while a comparison between experimental and calculated level energies, transition probabilities and the  $Q_s$  moment for the  $2_1^+$  state, for both approaches, is provided in Fig. 3. Note that the GTRM approach differs from the RTRM model of Davydov et al. [27,28] as it overcomes a number of limitations of the RTRM, such as irrotational moments of inertia [49], for example.

It is clear that the data are well reproduced. In particular, the strong coupling between  $K = 2$  and  $K = 0$  states, which manifests itself through a large  $2_2^+ \rightarrow 2_1^+$  matrix element, is borne out by the data as are the excitation energies of the  $2_2^+$  and  $3_1^+$  states. These observables and, in particular, the relatively large  $2_2^+ \rightarrow 2_1^+$  and small  $2_2^+ \rightarrow 0_1^+$  matrix elements, are strong indications of triaxial deformation. In fact, in the GTRM calculations, the  $\gamma$  deformation parameter has a value of  $\gamma = 29^\circ$  and a  $\beta_2$  deformation of  $\beta_2 = 0.31$ . The extracted gamma deformation for  $^{110}\text{Ru}$  is the closest to  $30^\circ$  of all candidate triaxial nuclei investigated with multi-step Coulomb excitation data. Hence, the present study establishes the possibility of triaxiality near the ground state for a region other than Os–Pt and, in many regards, makes  $^{110}\text{Ru}$  the best candidate for triaxiality to date. The HFB-GCM(GOA) calculations yield similar deformation parameters of  $\gamma = 26^\circ$  and  $\beta_2 = 0.29$  with fluctuations in gamma of the order of  $\sim 12^\circ$ , indicating a more shallow minimum in the potential energy surface as compared to the  $\gamma$ -rigid assumption of the GTRM. The present data do not, however, allow for the extraction of experimental  $\beta$  and  $\gamma$  shape parameters as the  $Q_s$  moment for the  $2_2^+$  level could not be determined and no sensitivity to the relative signs of the  $2_1^+ \rightarrow 0_1^+$ ,  $2_2^+ \rightarrow 0_1^+$  and  $2_2^+ \rightarrow 2_1^+$  matrix elements was found in the GOSIA fit. For the analysis, the adopted convention was that all in-band matrix elements and the one linking the  $2_2^+$  level to the ground state were chosen to be positive, while ones between bands were allowed to take positive or negative values. Nevertheless, all the available experimental evidence of Table 1 and Fig. 3 is supported by the results of calculations pointing to a significant role for triaxiality in this nucleus ( $\gamma \sim 30^\circ$ ), albeit with a degree of  $\gamma$  softness.<sup>1</sup> It is also worth remembering that beyond-mean-field calculations within the same framework also reproduce satisfactorily data on, for example, the neutron-rich Sr isotopes [53] and the neutron-deficient Kr [54,55] and Se isotopes [56] where shape changes and/ or shape coexistence have been observed. Similarly, the GTRM model has been found to successfully reproduce the extensive set of measured  $E2$  matrix elements for the candidate triaxial nuclei  $^{186-192}\text{Os}$  [51].

Furthermore, the spectroscopic quadrupole moment,  $Q_s$ , was determined for the  $2_1^+$  state to be  $Q_s = -83_{-29}^{+39} e \text{ fm}^2$ . The large uncertainty is due in part to (i) the limited sensitivity in the angular range ( $30^\circ$ – $75^\circ$ ) where the analysis could be performed (due to the lack of separation between different nuclei at lower angles and the lack of ToF information at backward angles), and to (ii) insufficient precision in the determination of some other transition probabilities in  $^{110}\text{Ru}$  (in particular that of the  $2_2^+ \rightarrow 2_1^+$  transition, which has a second-order effect on the excitation cross section of the  $2_1^+$  state). Nevertheless, the sign of the  $Q_s$  moment is determined and firmly establishes that  $^{110}\text{Ru}$  has a prolate shape near its ground state. While the  $Q_s$  measurement agrees within  $\sim 1.3 \sigma$  with the HFM-GCM(GOA) and GTRM results described above, it is in clear disagreement with the calculations of Ref. [57] within the D1N formulation of the Gogny energy density functional [14] (without the GCM(GOA) treatment) which predict a static oblate deformation for the  $^{108-112}\text{Ru}$  isotopic chain. Not all models give predictions for quadrupole moments, however, it is worth also pointing to recent calculations within the Cranked Skyrme–Hartree–Fock–Bogoliubov (CSHFB) framework [13]. In this work,  $^{110}\text{Ru}$  is determined to be triaxial with deformation of the same magnitude ( $\beta_2 = 0.16$  and  $\gamma = 25^\circ$ ) as those computed here. The quoted  $Q_t$  moment [13] translates into a  $Q_s$  value of  $-100 e \text{ fm}^2$ , which is also in agreement with the measured spectroscopic quadrupole moment,  $Q_s = -83_{-29}^{+39} e \text{ fm}^2$ .

In conclusion, a number of recent developments have proved vital to the success of this measurement. First post-acceleration of a  $^{110}\text{Ru}$  beam is reported, which, when coupled with the enhanced performance provided by the large angular sensitivity of the CHICO2 particle detector and the  $\gamma$ -ray tracking capabilities of the GRETINA array, provides direct evidence for of relatively rigid triaxial deformation near the ground state in a neutron-rich Ru isotope. The success of this measurement represents a technical milestone and paves the way for future studies involving unstable, neutron-rich refractory isotopes, where non-axial shapes and other intriguing shape phenomena are predicted to occur, in particular  $^{112}\text{Ru}$  where triaxiality is expected to reach a maximum in the Ru isotopic chain.

## Acknowledgements

This work was funded by the U.S. Department of Energy, Office of Science, Office of Nuclear Physics, under Contract No. DE-AC02-06CH11357 (ANL), No. DE-AC05-00OR22725 (ORNL), DE-SC0014442 (WU), No. DE-AC02-05CH11231 (LBNL, GRETINA), No. DE-AC52-07NA27344 (LLNL), No. DE-FG02-05ER41379 (Richmond) and by the US DOE National Nuclear Security Administration under grant number No. DE-NA0001801 (Richmond). EP-R acknowledges the financial support of DGAPA-UNAM under the PASPA program. The project has received partial funding from the National Science Centre of Poland under the Harmonia Programme grant No. DEC 2013/10/M/ST2/00427. This research used resources of ANL's ATLAS facility, which is a DOE Office of Science User Facility.

## References

- [1] D.J. Hartley, et al., *Phys. Rev. C* 80 (2009) 041304(R).
- [2] S.W. Odegard, et al., *Phys. Rev. Lett.* 86 (2001) 5866.
- [3] T. Koike, K. Starosta, P. Joshi, G. Rainovski, J. Timar, C. Vaman, R. Wadsworth, *J. Phys. G, Nucl. Part. Phys.* 31 (2005) S1741.
- [4] A. Bohr, B.R. Mottelson, *Nuclear Structure*, W. A. Benjamin, Inc., Reading, Ma, 1975.
- [5] V.I. Dimitrov, S. Frauendorf, F. Donau, *Phys. Rev. Lett.* 84 (2000) 5732.
- [6] C.Y. Wu, et al., *Nucl. Phys. A* 607 (1996) 178.
- [7] J. Srebrny, et al., *Nucl. Phys. A* 766 (2006) 25.
- [8] J. Srebrny, D. Cline, *Int. J. Mod. Phys. E* 20 (2011) 422.
- [9] K. Wrzosek-Lipska, et al., *Phys. Rev. C* 86 (2012) 064305.

<sup>1</sup> Not every model predicts triaxiality in  $^{110}\text{Ru}$ : the present results contradict an analysis within the framework of the interacting boson model [52], where no evidence for triaxial shapes was found.

- [10] P. Moeller, et al., *Phys. Rev. Lett.* 97 (2006) 162502.
- [11] P. Moeller, et al., *At. Data Nucl. Data Tables* 94 (2008).
- [12] H. Hua, et al., *Phys. Rev. C* 69 (2004) 014317.
- [13] C.L. Zhang, G.H. Bhat, W. Nazarewicz, J.A. Sheikh, Yue Shi, *Phys. Rev. C* 92 (2015) 034307.
- [14] F. Chappert, M. Girod, S. Hilaire, *Phys. Lett. B* 668 (2008) 420.
- [15] J.-P. Delaroche, et al., *Phys. Rev. C* 81 (2010) 014303.
- [16] K. Nomura, N. Shimizu, T. Otsuka, *Phys. Rev. C* 81 (2010) 044307.
- [17] K. Kumar, *Phys. Rev. Lett.* 28 (1972) 249.
- [18] D. Cline, *Annu. Rev. Nucl. Part. Sci.* 36 (1986) 681.
- [19] E. Cheifetz, R.C. Jared, S.G. Thompson, J.B. Wilhelmy, *Phys. Rev. Lett.* 25 (1970) 38.
- [20] J.A. Shannon, et al., *Phys. Rev. B* 336 (1994) 136.
- [21] Q.H. Lu, et al., *Phys. Rev. C* 52 (1995) 1348.
- [22] H. Hua, et al., *Phys. Lett. B* 562 (2003) 201.
- [23] C.Y. Wu, et al., *Phys. Rev. C* 73 (2006) 034312.
- [24] S.J. Zhu, et al., *Prog. Part. Nucl. Phys.* 59 (2007) 329.
- [25] J. Aysto, et al., *Nucl. Phys. A* 515 (1990) 365.
- [26] J.C. Wang, et al., *Phys. Rev. C* 61 (2000) 044308.
- [27] A.S. Davydov, G.F. Filippov, *Nucl. Phys.* 8 (1958) 237.
- [28] H. Toki, A. Faessler, *Z. Phys. A* 276 (1976) 35.
- [29] G. Gurdal, F.G. Kondev, *Nucl. Data Sheets* 113 (2012) 1315.
- [30] A. Faessler, W. Greiner, R.K. Sheline, *Nucl. Phys.* 70 (1965) 33.
- [31] H. Toki, A. Faessler, *Z. Phys. A* 276 (1976) 35.
- [32] J.B. Snyder, et al., *Phys. Lett. B* 723 (2013) 61.
- [33] R.C. Pardo, G. Savard, R.V.F. Janssens, *Nucl. Phys. News* 26 (2016) 5.
- [34] D.G. Jenkins, *Nat. Phys.* 10 (2014) 909.
- [35] S. Paschalis, I.Y. Lee, A.O. Macchiavelli, C.M. Campbell, M. Cromaz, S. Gros, J. Pavan, J. Qian, R.M. Clark, et al., *Nucl. Instrum. Methods A* 709 (2013) 44.
- [36] C.Y. Wu, D. Cline, A. Hayes, R.S. Flight, A.M. Melchionna, C. Zhou, I.Y. Lee, D. Swan, R. Fox, J.T. Anderson, *Nucl. Instrum. Methods A* 814 (2016) 6.
- [37] B. Bucher, S. Zhu, C.Y. Wu, R.V.F. Janssens, D. Cline, A.B. Hayes, et al., *Phys. Rev. Lett.* 116 (2016) 112503.
- [38] G. Savard, A. Levand, R. Pardo, R. Vondrasek, B. Zabransky, *JPS Conf. Proc.* 6 (2015) 010008.
- [39] G. Savard, S. Baker, C. Davids, A.F. Levand, E.F. Moore, R.C. Pardo, R. Vondrasek, B.J. Zabransky, G. Zinkann, *Nucl. Instrum. Methods B* 266 (2008) 4086.
- [40] T. Czosnyka, D. Cline, C.Y. Wu, *Am. Phys. Soc.* 28 (1983) 745.
- [41] J.B. Snyder, Ph.D. Thesis, Washington University, St Louis, 2014.
- [42] G. Mamane, et al., *Nucl. Phys. A* 454 (1986) 213.
- [43] S. Schoedder, et al., *Z. Phys. A* 352 (1995) 237.
- [44] R. Krucken, et al., *Phys. Rev. C* 64 (2001) 017305.
- [45] J.-P. Delaroche, J. Libert, M. Girod, *Phys. Rev. C* 60 (1999) 054301.
- [46] J. Dechargé, D. Gogny, *Phys. Rev. C* 21 (1980) 1568.
- [47] J.-F. Berger, M. Girod, D. Gogny, *Comput. Phys. Commun.* 63 (1991) 365.
- [48] J.M. Allmond, J.L. Wood, Generalized triaxial rotor model (GTRM) code, unpublished, 2005.
- [49] J.L. Wood, A.M. Oros-Peusquens, R. Zaballa, J.M. Allmond, W.D. Kulp, *Phys. Rev. C* 70 (2004) 024308.
- [50] W.D. Kulp, J.M. Allmond, P. Hatcher, J.L. Wood, et al., *Phys. Rev. C* 73 (2006) 014308.
- [51] J.M. Allmond, A.M. Oros-Peusquens, R. Zaballa, W.D. Kulp, J.L. Wood, *Phys. Rev. C* 78 (2008) 014302.
- [52] M. Boyukata, P.V. Isacker, I. Uluer, *J. Phys. G* 37 (2010) 105102.
- [53] E. Clément, et al., *Phys. Rev. Lett.* 116 (2016) 022701.
- [54] E. Clément, et al., *Phys. Rev. C* 75 (2007) 054313.
- [55] M. Girod, J.-P. Delaroche, A. Gorgen, A. Obertelli, *Phys. Lett. B* 676 (2009) 39.
- [56] J. Ljungvall, et al., *Phys. Rev. Lett.* 100 (2008) 102502.
- [57] J. Hakala, et al., *Eur. Phys. J. A* 47 (2011) 129.